PHYSICAL REVIEW B, VOLUME 63, 125402

Single-wall carbon nanotube diameter distributions calculated from experimental parameters

Henning Kanzow,* Christian Lenski, and Adalbert Ding
Technische Universiät Berlin, Optisches Institut, Strasse des 17. Juni 135, 10623 Berlin, Germany

(Received 18 May 2000; published 12 March 2001)

The growth of bundles of single-wall carbon nanotubes is explained by assuming a transition state, in which precipitated graphene sheets detach from the surface of a liquid catalyst particle, forming fullerenelike caps. The energetic situation of the transition state is considered as an equilibrium of the kinetic energy: the work of adhesion of the graphene sheet toward the catalytic particle and the strain energy associated with the cap formation. The tube diameter distributions depend only on their formation temperature range, the composition of the catalytic metal and carbon-containing particles, and the type of metal used. The calculated diameter distributions for different metal catalysts agree very well with the experimental data of arc and laser experiments of other groups. The observed increase of the tubes mean diameters with the formation temperature is also correctly reproduced by the simple model.

DOI: 10.1103/PhysRevB.63.125402 PACS number(s): 81.10.Aj, 81.05.Tp, 52.77.Bn, 68.03.Cd

I. INTRODUCTION

Since their discovery in 1993,[1,2] single-wall carbon nanotubes (SWCNT's) have attracted a great deal of interest from the scientific community due to their remarkable properties: They are conductors or semiconductors, depending on their helicity,[3] and can be used as transistors.[4] Their Young modulus reaches values of more than 1 TPa.[5] Their small dimensions allow them to be excellent atomic force microscope tips[6] and field emitters.[7] SWCNT's are traditionally produced by covaporization of pure carbon and a metal catalyst, either in an electric arc discharge[1,2,8–15] or by high power laser irradiation.[16–26] *In situ* studies of the formation of the tubes are still rare.[24,26] Thus it is not known how tube growth actually takes place. The models proposed for metal catalyzed SWCNT growth can be classified by the size of the catalytic metal containing particle.

(A) The catalytic particle is smaller than the SWCNT diameters: These models start from the carbon-metal gas phase: In the first place open fullerene structures in the shape of half bowls are formed near the plasma. ''Scooting'' small metal clusters or atoms hinder the closure of the bowls and further carbon atoms or units are incorporated, leading to tubular growth.[16,17,27]

(B) The catalytic particles are of the same size as or larger than the SWCNT diameters: The carbon and metal atoms condense at high temperatures to liquid droplets. Fullerenelike caps are either formed from segregated graphene sheets on the catalytic particle or are first generated in the gas phase and then attach to the particle surface. The subsequent segregated carbon atoms at the root of the caps are incorporated, leading to a single-wall tube growth.[8,9,15,25,28,29]

Several experimental observations strongly favor the root growth models B: Sea urchin and raftlike morphologies for SWCNT's attached to large catalytic particles have been observed for several metals and metal mixtures like Ce, Co, Gd, La, Ni, Ni/Co, Ni/Y, Rh/Pd, and Y.[8–10,14,18] Saito *et al.*[11] examined particles caught at different distances from the arc, and measured the corresponding local temperatures T: At a distance of 1.5 cm ($T = 1100\,^\circ\mathrm{C}$) only metal- and carbon-containing particles, but hardly any fibrous structures, were found. The products at 4 cm ($T = 650\,^\circ\mathrm{C}$), however, consisted of larger metal- and carbon-containing particles with ropes of SWCNT's directly attached to them. These rather low formation temperatures are also supported by recent experiments with pulsed lasers: Solids (e.g., nanotubes) were formed on a time scale between 1 ms and a few seconds after the pulse, when the plasma plume had cooled down considerably.[24,26] Within mechanism B, the question occurs of whether the necessary fullerenelike caps originate from fullerenes or fullerene fragments, which had been formed in the gas phase and became attached to the catalytic particle, or if the caps are formed from segregated graphene sheets on the particle surface. We believe that fullerenes are not directly used as building blocks of the SWCNT tips: C_{60} fullerenes are a typical by-product of the laser method. But the experimentally observed tube diameters are often much larger (0.9–1.7 nm) than the 0.7 nm corresponding to C_{60}.[18,20] Furthermore, there are several reports of SWCNT's produced by the interaction of gaseous carbon containing compounds like carbon monoxide or hydrocarbons with small metal particles. This method is called chemical vapor deposition (CVD).[30–33] It is difficult to imagine that fullerenes are involved in the formation of the SWCNT's in CVD experiments. If a single growth path is assumed for the CVD and plasma methods, a mechanism using fullerenes directly as a building block seems to be rather unlikely. CVD methods are much more widely known for the production of graphite fibers and multiwall carbon nanotubes (MWCNT's).[34–37] There are many similarities between the CVD and the plasma methods: The metal particles found in the product of the plasma methods have the same size as the ones found to be active in the CVD experiments.[36] Carbon-containing gases are present in both setups (e.g., fullerenes or hydrocarbons and carbon monoxide respectively). The temperature range of the formation of SWCNT's with CVD is $700–1200\,^\circ\mathrm{C}$,[30–33] the same as in the arc method.[11] MWCNT's can be also produced with plasma methods.[38,39] However, these structures certainly have a very different formation history, since metal catalysts are not needed for their generation. In the arc method MWCNT's are almost exclusively found in the inner core of the cathode deposit, where the electrode is hit by the arc, which implies very high formation temperatures. The diameters of these arc-grown MWCNT's are between 2 and 25 nm.[39] In the laser ablation method[20–22,24,26] as well as the arc method,[13] heating of the area around the plasma leads to an increase of the SWCNT mean diameters. The diameter distribution also strongly depends on the metal used as a catalyst in the plasma methods: Seraphin[9] showed histograms of the diameters of SWCNT's produced in a carbon-metal arc with either cobalt, iron, or nickel. She found that in soot samples (not the collaret) produced with iron and nickel most tubes were in the similar range of 0.7–1.0 nm, while in the sample produced with cobalt the distribution of the diameters was much broader, varying between 0.85 and 1.90 nm. These results are in agreement with the data of Saito *et al.*,[11] who observed mean diameters of 1.0–1.1 nm with iron, 1.1–1.2 nm with nickel, and 1.3–1.4 nm when using cobalt in the arc. In our recent theoretical paper we explained these diameter dependencies qualitatively.[29] We now show a simple way to evaluate our equations further and to calculate the diameter distributions.

II. GROWTH MODEL

The growth model follows the ''tradition'' of the diffusion model described by Tibbetts for generation of MWCNT's by the CVD method.[35] A similar model for SWCNT's was first proposed by Saito,[8] leaving open the question of where the necessary fullerenelike caps come from and what the state of the catalyst is. The catalytic particle is most likely in the liquid state: Macroscopic amounts of metal-carbon mixtures have eutectic melting temperatures of 1153, 1320, or 1327 °C for iron, cobalt, or nickel, respectively.[40] Under experimental conditions (plasma or CVD) melting temperatures are certainly strongly reduced because of the oversaturation of the metal particles with carbon[41] and the surface energy associated with the small dimensions.[42,43] Very low melting points between 600 and 700 °C for abnormally oversaturated solutions of carbon in the metals Fe, Ni, and Co were indeed reported by Krivoruchko and Zaikovskii, who studied the reaction of small metal particles with amorphous carbon.[44] We do not expect that carbide formation must be considered in the tube formation process for Fe, Ni, and Co. At the reaction temperatures these metals do not form stable carbides. That is, decomposition of Ni_3C occurs above 430 °C,[45] and that of Co_2C at about 400 °C.[46] Pure cementite (Fe_3C), however, is known not to promote the generation of nanofibers.[47] Solid carbide particles, frequently observed in plasma experiments together with pure metal particles, are therefore most likely formed at lower temperatures. The formation of SWCNT's is thought to occur at liquid particles consisting of a solution of metal and carbon at temperatures about 1000 °C. The possible reaction mechanism is presented in Fig. 1.

(1) The starting point for the SWCNT growth is a small liquid metal particle in the gas phase oversaturated with carbon. It may be in contact with a substrate (e.g., amorphous carbon segregated at higher temperatures). It can absorb extra carbon by decomposing carbon containing gas molecules (e.g., hydrocarbons, fullerenes, or fullerene fragments) on the surface of the particle and dissolve the carbon.

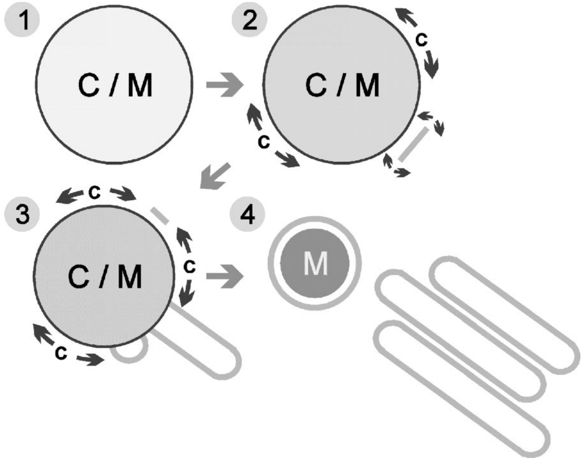

FIG. 1. Growth model for ropes of SWCNT's at liquid-metal particles. A hot temperature of the catalytic particle is indicated by a light color, and cooler particles are darker. Further explanation appears in the text.

(2) The oversaturation leads to a segregation of the carbon atoms. They move on or in the surface, and combine to form a first graphene layer, which grows continuously.

(3) If the system contains enough kinetic energy, the graphene plane is able to detach from the metal surface and form a fullerenelike cap. This process is preceded or accompanied by a rearrangement of the carbon atoms in the sheet in order to introduce the necessary six pentagons.[48] The addition of further carbon atoms at the edge of the cap makes it impossible for it to flatten out again. A SWCNT grows with a diameter corresponding to the initial cap size. Processes (1)–(3) will also occur on neighboring positions on the same particle. A rope of SWCNT's is generated.

(4) When the melt solidifies, a huge amount of carbon stored in the liquid particle is segregated at once, because much more carbon can be dissolved in a melt than in a solid. This can close the tips of the tubes and encapsulates the metal droplet.

III. ENERGY SITUATION OF THE TRANSITION STATE

A flat small graphene sheet is part of or attached to the surface of a liquid particle consisting of a solution of metal and carbon. Metal atoms are bonded to the sheet border to avoid dangling or highly strained bonds. The segregation of carbon atoms near the graphene sheet, and therefore the sheet growth, is thought to take place slowly compared with the average time needed for its transformation into a fullerenelike cap. For this transformation in-plane and out-of-plane movements of the carbon atoms are required, which we treat independently because the kinetic energies responsible for these movements are stored in different vibrational degrees of freedom.

(a) Out-of-plane: The central part of the graphene sheet has to lift off the catalytic particle (Fig. 2). This can only happen if the kinetic energy per area at the particle sheet interface [Eq. (3)] is high enough to overcome the work of

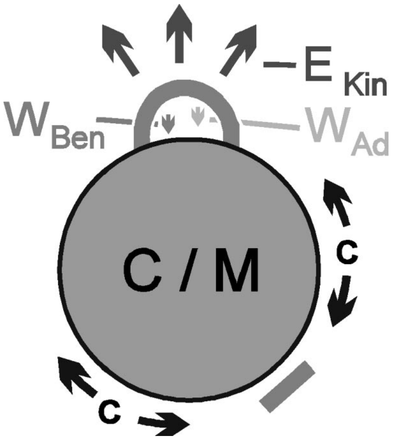

FIG. 2. Model of the transition state: A fullerene cap is formed from a graphene sheet on a catalytic particle.

adhesion. The excess energy is used for bending the sheet [Eq. (2)]. Equations (3)–(6), necessary to calculate Eq. (2), were discussed in our previous paper in detail.[29] Note that we had to correct Eq. (3). The parameter related to the type of metal used is a temperature-dependent function of the work of adhesion per area of graphite to the pure liquid metal $W_{Ad,M}$ [Eq. (5)]. If mixed metal catalysts are considered, a linear combination of the $W_{Ad,M}$ functions of the single metals is used. Equation (1) is new, and combines the available free energy for bending with the diameters of the fullerene caps. It derives from the fit function of the elastic theory of Tersoff[49] to the heat of formation data (approximately free energy of formation) of different-sized fullerenes calculated by Zhang *et al.*[50] The strain energy per area of a carbon atom in a fullerene (cap) is its free energy of formation (approximately the heat of formation) divided by the area it occupies minus the free surface energy (approximately that of graphite). The introduction of a simple equation like Eq. (1) for the strain energies of the caps is of course a strong idealization. But a detailed calculation of the strain energies of all possible nanotube tips is a rather hopeless approach. There are approximately 23 000 possibilities just to terminate the prominent (10,10) tube (approximately 9000, if the isolated pentagon rule is followed).[48] Our formulas imply that the strain energy of the fullerene cap is exclusively derived from the energy stored in the vibrational mode perpendicular to the particle sheet interface. In our calculations we arbitrarily set the angle between the cap edge and the particle surface to 90°. If the 90° angle is not reached because of a lack of kinetic energy, the cap is thought to flatten out again, and the graphene sheet continues to grow to a larger size. The ‘‘decoration’’ of the graphene sheet edge with metal atoms is an image to avoid any contribution of extra binding forces or tension between the cap and the particle surface during cap formation. These metal atoms are itself are part of the liquid particle surface:

$$W_{Ben} \approx \frac{\Delta H_f}{A_C} - 2E_{S,G} = \frac{e}{\pi d^2}\left[A + B\ln\left(\frac{\pi d^2}{A_C}\right)\right] - 2E_{S,G} \tag{1}$$

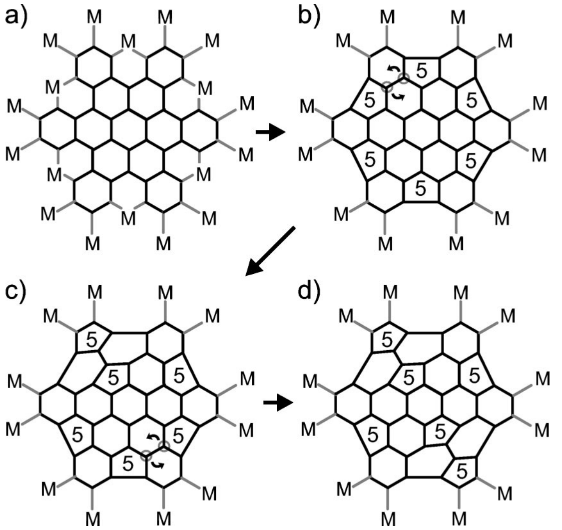

FIG. 3. A flat graphene sheet is converted into a round fullerene cap by introducing six pentagons from the side and moving them with two Stone-Wales rearrangements.

$$W_{Ben} = E_{kin} - W_{Ad}, \tag{2}$$

$$E_{kin} = \frac{kT}{A_C} + \frac{kT}{A_{MC}}, \tag{3}$$

$$A_{MC} \approx [X_C a_{C-C} + (1-X_C) a_{M\text{-}M}]^2, \tag{4}$$

$$W_{Ad} \approx X_C W_{Ad,G} + (1-X_C) W_{Ad,M}, \tag{5}$$

$$W_{Ad,G} \approx 2E_{S,G} \tag{6}$$

Equations (1)–(6) use the following parameters:

A_C: area of a carbon atom in graphite,
A_{MC}: area of an atom in the surface of the catalytic particle,
$a_{M\text{-}M}$: atom distance in the pure metal M,
$a_{C\text{-}C}$: bond length in graphite,
d: cap (tube) diameter,
A,B: constants from the fit in Fig. 3 of Ref. 49,
$E_{S,G}$: free surface energy of graphite per area,
ΔH_f: heat of formation for an atom in a fullerene cage,
E_{kin}: kinetic energy per area at the interface between the graphene sheet and the particle,
X_C: molefraction of carbon in the surface of the catalytic particle,
T: temperature,
W_{Ad}: work of adhesion per area of graphite toward the catalytic particle,
$W_{Ad,G}$: work of adhesion per area of graphite to liquid carbon,
$W_{Ad,M}$: work of adhesion per area of graphite to the metal M,
W_{Ben}: work of bending per area.

(b) Six pentagons have to be introduced into the graphene network, which are characteristic for fullerenelike caps. These pentagons can be introduced from the sides. An example is illustrated in Fig. 3: Figure 3(a) shows a highly symmetric flat graphene sheet (C_{48}). The otherwise unsaturated dangling bonds are decorated with metal atoms. If the metal atoms bound to two carbon atoms are removed, six pentagons are created at the border of the sheet [Fig. 3(b)]. Pentagons at the sheet edge can also consist of one or two metal atoms and the corresponding number of carbon atoms. The cap in Fig. 3(b) is rather obtuse. But all kinds of SWCNT tips,[10] especially round ones, are experimentally observed. Figures 3(c) and 3(d) show how the structure in Fig. 3(b) can be transformed into a round fullerene cap. Two pentagons from the edge ''diffuses'' into the center of the cap by just two in plane switches of C_2 units. These transformations are often called Stone-Wales transformations, after the scientist who used them first for explaining the isomerization reactions of fullerenes.[51] But these kinds of transformations were discussed much earlier in connection with the carbon diffusion in graphite.[52,53] Calculations show that the energetic barriers for ''pure'' Stone-Wales transformations are as high as 5–7 eV in flat graphene sheets as well as in SWCNT's (Ref. 54) and fullerenes.[55] Unfortunately there are no calculations on the effects of transition metals, which certainly have a much greater potential to catalyze these rearrangements. The time available for the nucleation of fullerene caps is not known, but it should be significantly lower than a time scale in the order of a second associated with the growth of SWCNT's.[26] Activation energies of 5–7 eV surely inhibit the switches discussed above at reaction temperatures of approximately 1000 °C. (The corresponding reaction rate can be estimated with the Arrhenius equation.[54]) However, the barrier can be strongly lowered by strain,[54] or by catalytic effects of the presence of extra carbon or hydrogen atoms.[55] Experiments with polycyclic aromatics such as aceanthrylene, acephenanthrylene and fluoranthene, show that 5-6-ring rearrangements of the carbon skeleton are performed rapidly at 1100 °C.[56] To resume this part, only a few in-plane movements of carbon atoms are necessary to create a fullerenelike cap from a flat graphene sheet. It is not absolutely clear (but seems likely), that the activation barriers are sufficiently low so that the rearrangements of the sheet can be performed fast enough. In our model it is assumed that low activation energy paths for the rearrangement exist. The in-plane movements of the carbon atoms are therefore not considered further in our calculation.

IV. PROCEDURE OF CALCULATION

Concerning the arc experiments the diameter distribution of the tubes was only calculated for tubes in the ''soot'' (and not in the ''collaret''), because we just know the formation temperature range for the tubes in the soot given by Saito *et al.* to be 650–1100 °C.[11] The other necessary parameter is the carbon content at the surface of the catalytic particle. The original composition of the evaporated anode material usually contains only 1 at. % of metal and 99 at. % of carbon. The particles formed from the gas phase will have similar compositions. Then the carbon is transformed into nanotubes, and the metal accumulates in the particle. The final composition is of almost pure metal. Therefore, we set the parameter range for the carbon content to be between 0 to 1. The temperature and the carbon content ranges were divided into 51 equidistant values each. In order to calculate the diameters we have to compose pairs of carbon content and temperature values. We used the simplest approximation, that all combinations have the same probability: Thus every carbon content value was combined with every temperature value. For the resulting 2601 combinations the diameters were (numerically) calculated using Eqs. (1)–(6). We also calculated the diameter distribution corresponding to a pure carbon catalyst particle for the temperature ranges 650–1100 °C (formation temperature of SWCNT's) and 2500–3000 °C (assumed formation temperature of arc-produced MWCNT's in agreement with Ref. 57). This was done to check, if our model can also explain the growth of MWCNT's in the arc experiment. In the laser experiments the lower temperature limit is not 650 °C, but set by the oven temperature, which we used in our calculation. As the upper limit we chose the same value as in the arc experiments, though one should keep in mind that SWCNT's can grow at slightly higher temperatures.[20]

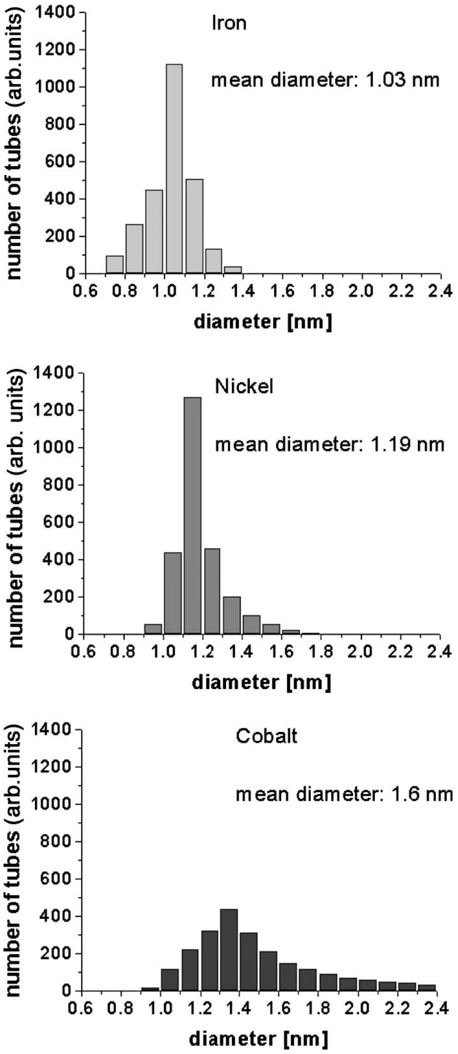

FIG. 4. Calculated SWCNT diameter distributions in the soot of an electric arc experiment with single-metal catalysts.

V. RESULTS AND DISCUSSION

Figure 4 shows the results for the pure metal catalysts Fe, Ni, and Co. The obtained tube diameter distributions with the single metal catalysts fit very well to the experimental data of Seraphin[9] and Saito *et al.*:[11] The mean diameters of the tubes made with iron and nickel catalysts have the same values as in the experiments (1.0 and 1.2 nm, respectively). Their narrow diameter distributions are also reproduced. The model predicts a larger mean diameter and also a broader diameter distribution for the cobalt catalyst. These characteristics are indeed found in the experiments. But the calculated distribution shows too large a tail on the larger diameter side, which was not found in the experiments. This might be due to the rather poor work of adhesion functions we had to use.[29] However, the maximum of the diameter distribution coincides (as for the iron and nickel catalysts) with the mean diameters observed by Saito *et al.* and Seraphin. For pure carbon as the catalyst, we calculated SWCNT mean diameters of 1.08 nm for the temperature range of 650–1100 °C with a slightly narrower diameter distribution than in the case of iron. For the 2500–3000 °C temperature range the mean diameter was reduced to 0.57 nm. The corresponding diameter distribution was extremely narrow. The diameters of arc-grown MWCNT's are much larger than the results of our calculations. The formation of these tubes certainly takes place in a quite different way[57] from the growth model we present in this paper. Figure 5 shows the diameter distributions with the mixed metal catalysts Fe/Ni, which were calculated for the laser experiments for oven temperatures of 780 and 1000 °C. The corresponding tube diameters observed with TEM by Bandow *et al.* (Fig. 2 in Ref. 21) are included in Fig. 5 as gray squares. The original data were normalized in order to compare the results with our calculations. The obtained diameter distributions are in good agreement with the experiments: The increase of the mean diameter with the formation temperature is correctly reproduced. Furthermore the width of the distributions are very similar to the experimentally observed ones.

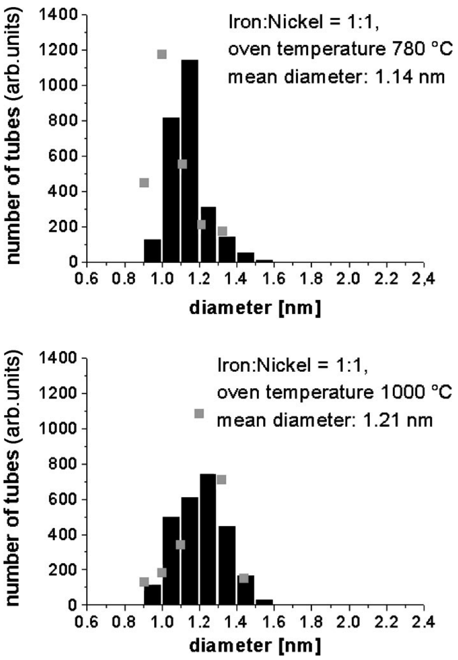

FIG. 5. Calculated SWCNT diameter distributions in the product of a laser experiment with an iron/nickel 1/1- mixture as the catalyst, and oven temperatures 780 and 1000 °C, respectively. The scaled abundances of diameters observed with TEM by Bandow *et al.* (Fig. 2 in Ref. 21) are included as gray squares for comparison.

As mentioned above, the calculated diameter distributions for the metal catalyzed SWCNT's are in very good agreement with the experiments. This is a surprising result, because we had to introduce many rough approximations to perform our calculations with our simple model. The values for the temperatures and the work of adhesion we use certainly have some experimental uncertainties. Some of our assumptions, e.g., a low-energy path for the arrangement of the atoms, have not yet been confirmed. On the other hand, our results strongly support the view that nanotube tips are created at a catalytic particle and that SWCNT diameter distributions are controlled by the kinetic energy present in the system and the work of adhesion of the catalytic material toward the graphene sheet.

VI. CONCLUSION

We have found a method to calculate the diameter distributions of SWCNT's grown with laser and electric arc techniques. The crucial parameter for the diameter dependency on the catalytic metal used in the plasma methods is the work of adhesion of the metal toward graphite at reaction temperatures. The obtained diameter distributions for iron, nickel, and cobalt catalysts, and their mixtures, are in good agreement with the experimental observations of other groups. The model also explains the diameter dependency on the oven temperature in the laser experiment. This work may have an impact on the development of more detailed (e.g., on molecular-dynamics-based) models. For the time being it is a useful tool, which helps to find adequate reaction parameters, if certain diameter distributions are required for special applications.

---

*Present address: GDPC, Université Montpellier II, CC26, 34095 Montpellier Cédex 05, France; Fax: ++33 (0)467 14522504; Email: henning@gdpc.univ-montp2.fr

[1] S. Iijima and T. Ichihashi, Nature (London) **363**, 603 (1993).

[2] D.S. Bethume, C.H. Kiang, M.S. de Vries, G. Gorman, R. Savoy, J. Vazques, and R. Beyers, Nature (London) **363**, 605 (1993).

[3] R. Saito, M. Fujita, G. Dresselhaus, and M.S. Dresselhaus, Appl. Phys. Lett. **60**, 2204 (1992).

[4] S.J. Tans, A.R.M. Verschueren, and C. Dekker, Nature (London) **393**, 49 (1998).

[5] A. Krishnan, E. Dujardin, T.W. Ebbesen, P.N. Yianilos, and M.M.J. Treacy, Phys. Rev. B **58**, 14 013 (1998).

[6] S.S. Wong, A.T. Woolley, T. Wang Odom, J.-L. Huang, P. Kim, D.V. Vezenov, and C.M. Lieber, Appl. Phys. Lett. **73**, 3465 (1998).

[7] Y. Saito, K. Hamaguchi, T. Nishino, K. Hata, K. Tohji, A. Ka-

suya, and Y. Nishina, Jpn. J. Appl. Phys. **36**, L1340 (1997).

[8] Y. Saito, Carbon **33**, 979 (1995).

[9] S. Seraphin, J. Electrochem. Soc. **142**, 290 (1995).

[10] Y. Saito, K. Kawabata, and M. Okuda, J. Phys. Chem. **99**, 16 076 (1995).

[11] Y. Saito, T. Koyama, and K. Kawabata, Z. Phys. D: At., Mol. Clusters **40**, 421 (1997).

[12] C. Journet, W.K. Maser, P. Bernier, A. Loiseau, M. Lamy de la Chapelle, S. Lefrant, P. Deniard, R. Lee, and J.E. Fischer, Nature (London) **388**, 756 (1997).

[13] M. Takizawa, S. Bandow, T. Torii, and S. Iijimal, Chem. Phys. Lett. **302**, 146 (1999).

[14] C. Journet, Ph. D. thesis, Université Montpellier II, 1999.

[15] A. Leauseau and F. Willaime, Appl. Surf. Sci. **164**, 227 (2000).

[16] T. Guo, P. Nikolaev, A. Thess, D.T. Colbert, and R.E. Smalley, Chem. Phys. Lett. **243**, 49 (1995).

[17] A. Thess, R. Lee, P. Nikolaev, H. Dai, P. Petit, J. Robert, C. Xu, Y.H. Lee, S.G. Kim, A.G. Rinzler, D.T. Colbert, G. Scuseria, D. Tomanek, J.E. Fischer, and R.E. Smalley, Science **273**, 483 (1996).

[18] L.-C. Qin and S. Iijima, Chem. Phys. Lett. **269**, 65 (1997).

[19] W.K. Maser, E. Munoz, A.M. Benito, M.T. Martnez, G.F. de la Fuente, Y. Maniette, E. Anglaret, and J.-L. Sauvajol, Chem. Phys. Lett. **292**, 587 (1998).

[20] A.G. Rinzler, J. Liu, H. Dai, P. Nikolaev, C.B. Huffman, F.J. Rodriguez-Macas, P.J. Boul, A.H. Lu, D. Heymann, D.T. Colbert, R.S. Lee, J.E. Fischer, A.M. Rao, P.C. Eklund, and R.E. Smalley, Appl. Phys. A: Mater. Sci. Process. **76**, 29 (1998).

[21] S. Bandow, S. Asaka, Y. Saito, A.M. Rao, L. Gregorian, E. Richter, and P.C. Eklund, Phys. Rev. Lett. **80**, 3779 (1998); E. Anglaret, S. Rols, and J.-L. Sauvajol, *ibid.* **81**, 4780 (1998).

[22] A.M. Rao, S. Bandow, E. Richter, and P.C. Eklund, Thin Solid Films **331**, 141 (1998).

[23] H. Kataura, A. Kimura, Y. Ohtsuka, S. Suzuki, Y. Maniwa, T. Hanyu, and Y. Achiba, Jpn. J. Appl. Phys. **37**, L616 (1998).

[24] F. Kokai, K. Takahashi, M. Yudosaka, and S. Iijima, J. Phys. Chem. B **103**, 4346 (1999).

[25] H. Kataura, Y. Kumazawa, Y. Maniwa, Y. Ohtsuka, R. Sen, S. Suzuki, and Y. Achiba, Carbon **38**, 1691 (2000).

[26] A.A. Puretzky, D.B. Geohegan, X. Fan, and S.J. Pennycook, Appl. Phys. A: Mater. Sci. Process. **70**, 153 (2000).

[27] Y.H. Lee, S.G. Kim, and D. Tomanek, Phys. Rev. Lett. **78**, 2393 (1997).

[28] A. Maiti, C. Brabec, and J. Bernholc, Phys. Rev. B **55**, R6097 (1997).

[29] H. Kanzow and A. Ding, Phys. Rev. B **60**, 11 180 (1999).

[30] H. Dai, A.G. Rinzler, P. Nikolaev, A. Thess, D.T. Colbert, and R.E. Smalley, Chem. Phys. Lett. **260**, 471 (1996).

[31] J.H. Hafner, M.J. Bronikowski, B.R. Azamiam, P. Nikolaev, A.G. Rinzler, D.T. Colbert, and R.E. Smalley, Chem. Phys. Lett. **296**, 195 (1998).

[32] H.M. Cheng, F. Li, G. Su, H.Y. Pan, L.L. He, X. Sun, and M.S. Dresselhaus, Appl. Phys. Lett. **72**, 3282 (1998).

[33] J.-F. Colomer, Ph.D. thesis, Université Namur, 2000.

[34] A. Oberlin, M. Endo, and T. Koyama, J. Cryst. Growth **32**, 335 (1976).

[35] G.G. Tibbetts, J. Cryst. Growth **66**, 632 (1984).

[36] N.M. Rodriguez, J. Mater. Res. **8**, 3233 (1993).

[37] A. Fonseca, K. Hernadi, P. Piedigrosso, J.-F. Colomer, K. Mukhopadhyay, R. Doome, S. Lazarescu, L.S. Biro, P. Lambin, P.A. Thiry, D. Bernaerts, and J.B. Nagy, Appl. Phys. A: Mater. Sci. Process. **67**, 11 (1998).

[38] S. Iijima, Nature (London) **354**, 56 (1991).

[39] P.M. Ajayan and T.W. Ebbesen, Rep. Prog. Phys. **60**, 1025 (1997).

[40] T. B. Massalski, *Binary Alloy Phase Diagrams* (ASM International, Metals Park, OH, 1996).

[41] P. W. Atkins, *Physikalische Chemie* (VCH, Weinheim, 1990), p. 180.

[42] H. Kanzow, Ph. D. thesis, Technische Universität Berlin, 2000.

[43] K.F. Peters, J.B. Cohen, and Y.-W. Chung, Phys. Rev. B **57**, 13 430 (1998).

[44] O.P. Krivoruchko and V.I. Zaikovskii, Kinet. Katal. **39**, 561 (1998).

[45] D.L. Leslie-Pelecky, X.Q. Zhang, S.H. Kim, M. Bonder, and R.D. Rieke, Chem. Mater. **10**, 164 (1998).

[46] T.J. Konno and R. Sinclair, Acta Metall. Mater. **42**, 1231 (1994).

[47] R.T.K. Baker, J.R. Alonzo, J.A. Dumesic, and D.J.C. Yates, J. Catal. **77**, 74 (1982).

[48] G. Brinkmann, P.W. Fowler, D.E. Manolopoulos, and A.H.R. Palser, Chem. Phys. Lett. **315**, 335 (1999).

[49] J. Thersoff, Phys. Rev. B **46**, 15 546 (1992).

[50] B.L. Zhang, C.H. Xu, C.Z. Wang, C.T. Chan, and K.M. Ho, Phys. Rev. B **46**, 7333 (1992).

[51] A.J. Stone and D.J. Wales, Chem. Phys. Lett. **128**, 501 (1986).

[52] G.J. Dienes, J. Appl. Phys. **23**, 1194 (1952).

[53] M.A. Kanter, Phys. Rev. **107**, 655 (1957).

[54] M.B. Nardelli, B.I. Yakobson, and J. Bernholc, Phys. Rev. B **57**, R4277 (1998).

[55] B.R. Eggen, M.I. Heggie, G. Jungnickel, C.D. Latham, R. Jones, and P.R. Briddon, Science **272**, 87 (1996).

[56] L.T. Scott and N.H. Roelofs, J. Am. Chem. Soc. **109**, 5461 (1986).

[57] J.-C. Charlier, A. De Vita, X. Blase, and R. Car, Science **275**, 646 (1997).